Rock Mechanics and Rock Engineering (2022) 55:3385–3397
https://doi.org/10.1007/s00603-022-02815-w

ORIGINAL PAPER

The Effect of Normal Load Oscillation Amplitude on the Frictional Behavior of a Rough Basalt Fracture

Wengang Dang[1] · **Heinz Konietzky**[2]

Received: 13 July 2021 / Accepted: 7 February 2022 / Published online: 22 February 2022

Abstract

Quantifying the changes of frictional strength during dynamic normal loading is significant for investigations of joint and fault interaction as well as earthquake triggering. The frictional character of a natural basalt rock fracture with a rough surface is investigated by conducting well-controlled, repeatable direct shear experiments using a large-scale dynamic shear box equipment. Normal force oscillations, simulating a dynamic normal force, are applied to the fractured basalt sample. Simultaneously, a shear force acts on the lower block of the sample which provides a constant slip rate. The frictional behavior is investigated by applying a normal load with oscillation amplitude from 0 up to 80% of the initial normal load. Experimental results showed that the dynamic disturbance decreases the friction of the rock fracture, the minimum friction reduces with rising normal load oscillation amplitude. The dynamic disturbance enhances the maximum shear force under the smaller normal load oscillation amplitude. When the normal load oscillation amplitude exceeds a critical point, the maximum shear force reduces, even reaching "negative" values. Moreover, a phase difference (D1) is identified between peak normal load and peak shear load with peak normal load leading. There is also a phase difference (D2) between peak normal load and peak apparent dynamic friction coefficient. The phase difference of D1 rises with rising normal load oscillation amplitude, decreases with shearing, while, relative phase lag of D2 keeps constant. Our results confirm that dynamic normal force can both enhance and reduce the stability of a steadily slipping fracture depending on the normal force oscillation amplitude.

Highlights

- Dynamic normal load can both enhance and reduce the stability of the steadily creeping faults dependent on the normal load oscillation amplitude.
- A critical normal load oscillation amplitude is confirmed to judge the frictional strengthening or frictional weakening of the creeping rock fracture.
- A time difference between peak normal force and peak shear force with normal force ahead is confirmed.

Keywords Oscillation amplitude · Phase difference · Friction · Normal load oscillation-induced strengthening/weakening

List of Symbols

A	Normal load oscillation amplitude
A^*	Critical normal load oscillation amplitude
F_{sd}	Dynamic normal load
F_N	Initial normal load
f	Normal load oscillation frequency
t	Time
F_s	Shear force
ΔF_{s1} ΔF_{s2}	Variation of shear force
$\Delta\mu_{d1}$ $\Delta\mu_{d2}$	Variation of dynamic coefficient of friction
Δd_1 Δd_2	Variation of vertical displacement
μ_{ss}	Initial friction coefficient
μ_d	Dynamic friction coefficient
μ_{dmax}	Maximum value of dynamic friction coefficient in a cycle

✉ Wengang Dang
dangwg@mail.sysu.edu.cn

[1] School of Civil Engineering, Sun Yat-Sen University, and Southern Marine Science and Engineering Guangdong Laboratory (Zhuhai), Zhuhai 519082, China

[2] Geotechnical Institute, TU Bergakademie Freiberg, Gustav-Zeuner-Straße 1, 09599 Freiberg, Germany

μ_{dmin}	Minimum value of dynamic friction coefficient in a cycle
D1	Time difference between normal stress and shear stress
D2	Time difference between normal stress and apparent friction coefficient
D3	Time difference between normal stress and vertical displacement
E	Energy consumption
Ɛ	Normalized normal load oscillation amplitude, i.e., A/F_N
u	Slip length
u_{max}	Maximum slip length
v	Slip rate
Z_i	Asperity height
n	Number
Δx	Interval of data points

1 Introduction

Periodic loading caused by ocean waves, earth tides or earthquakes are complicated dynamic natural movements connected with dynamic stresses (Stein 1999; Julian 2000; Candela et al. 2014; Wei et al. 2013, 2015; Zhou et al. 2020; Xie et al. 2021). Under certain conditions, shear and normal loads on surrounding fractures are altered and slipping along rock fractures under dynamic normal stresses happens (Stein 1999; Candela et al. 2014). To investigate the slip behavior of rock joints/fractures exposed to dynamic normal load disturbance, several researchers performed corresponding shear experiments (Linker and Dieterich 1992; Cochard et al. 2000, 2003, 2021; Rice et al. 2001; Hong and Marone 2005; Konietzky et al. 2012; Smith et al. 2015; Kilgore et al. 2012, 2017; Molinari and Perfettini, 2017; Dang et al. 2016, 2018; Meng et al. 2018; Webber et al. 2018; Aiken et al. 2018; Mighani et al. 2019; Gong et al. 2020, 2021; Ji et al. 2021).

Normal stress disturbance weakens the shear stress of rock fractures (Marone, 1998; Rice, 2006; Sheng et al. 2020; Mei et al. 2021), and the evolution of friction due to a sudden increase in normal stress obeys a three-stage development. Hobbs and Brady (1985), Olsson (1988) carried out double shear experiments on gabbro and welded tuff responding to sudden variations in normal load. The shear stress alters significantly at the beginning followed by an exponential pattern. Linker and Dieterich (1992) performed double shear tests on Westerly granite under a step-wise load variation. They observed that the changes in shear stress are divided into three stages, an instantaneous increase in the first stage, fast linear increase in the second stage, and reaching a constant value in the third stage. Hong and Marone (2005) conducted slip experiments on Westerly granite with different gouge fillings in the fractures. The shear stress also changes when normal stress alters according to a multi-stage behavior. Kilgore et al. (2012, 2017) investigated the shear behavior on granite exposed to dynamic disturbance. A gradual, approximately exponential variation in shear stress is reported. Moreover, the memory effect is pronounced (Prakash, 1998; Bureau et al. 2000). Dang et al. (2021) preformed direct shear tests on basalt samples with different slip rates. A critical slip rate is reported, which induces normal load oscillation-induced weakening or normal load oscillation-induced strengthening under dynamic normal load conditions.

Boettcher and Marone (2004), and Dang et al. (2017, 2018) investigated the frictional response of oscillating force amplitudes acting on planar fracture surfaces. Boettcher and Marone (2004) varied the normalized oscillation amplitude from 1 to 10%. Their work proved that larger oscillation amplitude produces a pronounced reduction in shear strength. Dang et al. (2018) varied the normalized oscillation amplitude from 11 to 67%, and reported that the minimum friction coefficient decreases with increasing oscillation amplitude. Moreover, a distinct phase difference between normal load and shear load with normal load leading is documented, where the relative phase difference increases with rising oscillation amplitude. Dang et al. (2020) investigated the cyclic shear response of artificial smooth fractures exposed to normal load oscillations. They found that normal force oscillation amplitudes, shear displacement amplitudes, normal force oscillation frequencies, shear direction reverse frequencies, and initial normal load levels are not linked to the maximum apparent coefficient of friction.

Natural rock fractures have typically rough surfaces. Planar/flat rock fracture surfaces are very rare in nature. However, most of the earlier studies on the slip behavior under dynamic normal forces concentrate on planar rock fractures (Hobbs and Brady, 1985; Hong and Marone, 2005; Dang et al. 2016, 2017, 2018). For planar rock fractures, the patterns of shear force and dilation are nearly the same in the stable slipping stage. Without consideration of the roughness of fracture surfaces, the understanding of the dynamic fracture strengthening/weakening is quite limited.

2 Experimental Methodology

The slip experiments were performed on a rough basalt rock joint using a dynamic shear equipment (Fig. 1a, Konietzky et al. 2012) at temperature of approximately 20 ℃ and nominal humidity of approximately 40%. The dynamic shear equipment consists of two hydraulic loading systems, which provides a constant slip rate and a periodic normal force. Shear and normal displacements are measured by linear

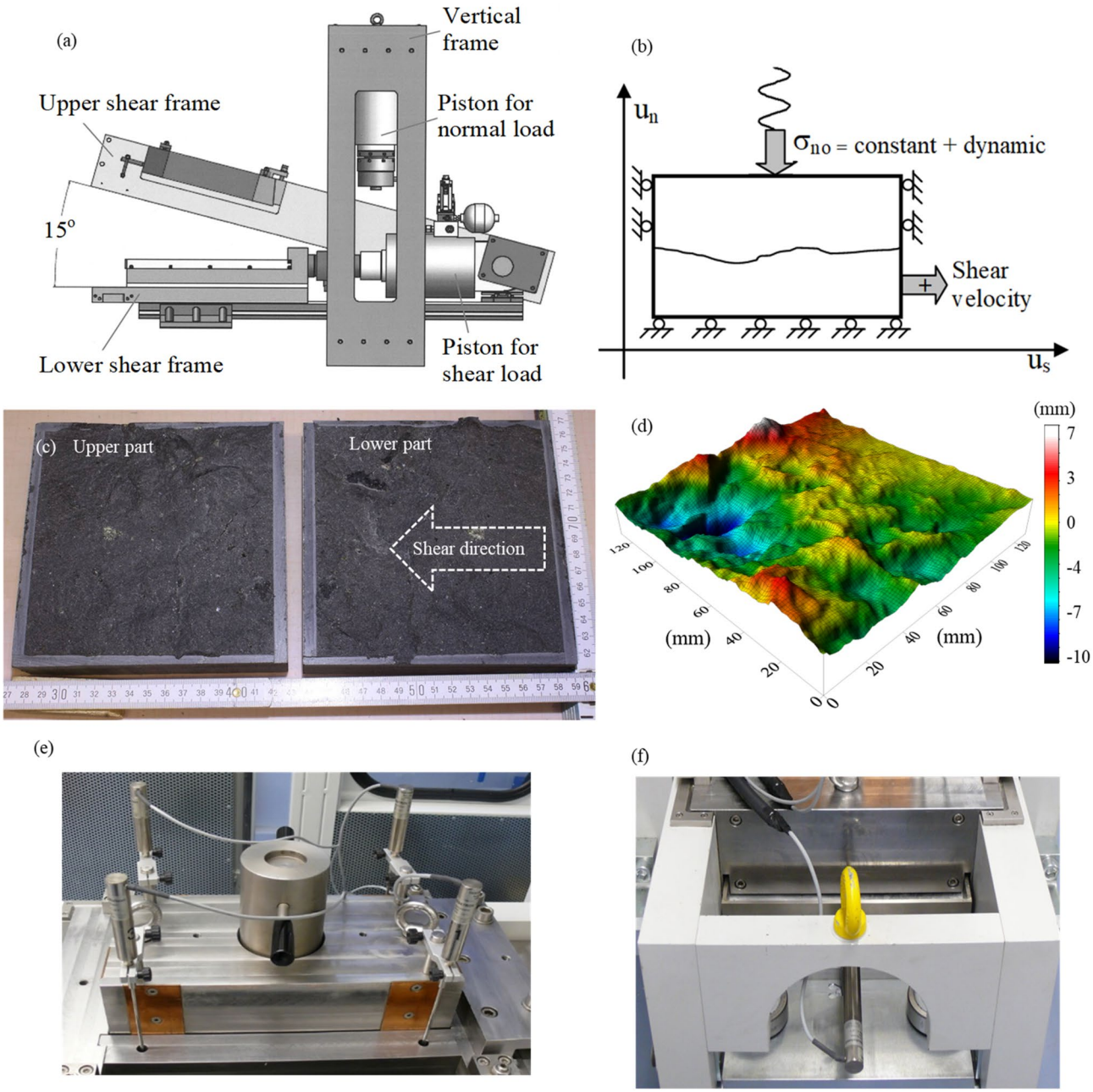

Fig. 1 **a** Scheme of equipment (Konietzky et al. 2012). **b** Schematic of slip experiment via periodical load with a constant slip rate (Dang et al. 2016). **c** Basalt rock showing the rough fracture surfaces. **d** Scanned fracture topography before the experiment, **e** vertical LVDTs **f** horizontal LVDT

variable differential transformers (LVDTs) with an accuracy of 0.001 mm (Fig. 1e, f). All measured data are sampled with rate of 100 Hz.

The rough basalt fracture was obtained by splitting an intact basalt block with a size of $150 \times 150 \times 100$ mm^3 (length × width × height). A pre-cut groove with a depth of 10 mm was created at the middle part of the sample using a motor saw. Then the pre-cut groove block is sheared using a uniaxial test machine, and the fracture surface is created nearly at the middle part of the rock sample. The effective contact area was 130×130 mm^2 (length × width) (Fig. 1c, d). Upper and lower surfaces matched almost completely. The intact basalt samples showed a uniaxial compressive strength of 220 MPa, and a uniaxial tensile strength of 16 MPa.

To carry out repeated experiments with the same rough surface, we adopted a relatively low initial normal force to guarantee the surface asperities are maintained almost

Table 1 Laboratory test programs

Series	F_N (kN)	f(Hz)	A (kN)	u_{max} (mm)	v (mm/min)	A/F_N (%)
1	50	0	0	5	5	0
2	50	0.5	10	5	5	20
3	50	0.5	20	5	5	40
4	50	0.5	25	5	5	50
5	50	0.5	30	5	5	60
6	50	0.5	40	5	5	80

$f=0$ means: the experiment was performed under constant normal load

unbroken during these tests. Tests were performed with an initial normal force of 50 kN, a slip velocity of 5.0 mm per minute, and a maximum slip length (u_{max}) of 5.0 mm. Each test lasted for 60 s. As shown in Fig. 1b, the superimposed oscillating normal load was governed by a sinusoidal wave (Eq. 1), with oscillating amplitudes of 0, 10, 20, 25, 30, and 40 kN, respectively. The oscillating amplitude of 0 kN means that the slip experiment was performed under constant normal load conditions. The normal load oscillation frequency was 0.5 Hz. The experimental plan is shown in Table 1. All six experiments were performed with dynamic normal load amplitude changes ranging from 0 to 80% (A/F_N). The fracture surfaces were scanned before and after the tests using a 3D scanner. The whole experiments lasted for several hours, during which temperature and humidity were kept nearly constant, so that temperature-humidity effects were neglected.

$$F_d = A\sin(2\pi ft) \tag{1}$$

3 Experimental Results

The surfaces of the rock fracture were scanned before and after the test by the 3D scanner "z-Snapper" (Fig. 2a), with an accuracy of 0.001 mm. The topography of the rough surface before and after the experiment of the fractures is shown in Fig. 2b. According to Tse and Crude (1979) law (Eqs. 2 and 3), joint roughness coefficient (JRC) and root mean square slope Z_2 were 0.260 and 13.2 before the test, and 0.257 and 13.0 after the test, respectively, which proves that the asperities of the fractures experience only very small degeneration. Based on the shear strength criterion proposed by Barton and Choubey (1977), the slight reduction of JRC has little effect on the shear strength.

$$Z_2 = \left[\frac{1}{(n-1)(\Delta x)^2}\sum_{i=1}^{n-1}\left(Z_{i+1}-Z_i\right)^2\right]^{\frac{1}{2}} \tag{2}$$

$$\mathrm{JRC} = 32.2 + 32.47\log Z_2 \tag{3}$$

Figure 3 presents details of the slip behavior under constant and dynamic normal forces. Shear force, friction coefficient, and dilation showed periodical changes along with periodical changes in normal force. The changing patterns of shear force, friction coefficient and dilation were significantly influenced by normal load oscillation amplitude and shear displacement. Taking A = 30 kN for example: Fig. 4 illustrates the methodology used to analyze the measured frictional response. Six quantities were investigated for each cycle: (1) shear force variation during normal load oscillations, ΔF_{s1} and ΔF_{s2}; (2) coefficient of friction variation during normal load oscillations, $\Delta\mu_{d1}$ and $\Delta\mu_{d2}$; (3) normal displacement variation during normal load oscillations, Δd_1 and Δd_2; (4) phase lag, D1 and D1', which are defined as phase lag between peaks and valleys in normal force and shear force; (5) phase lag, D2 and D2', which are defined as phase lag between peaks and valleys in normal force and actual coefficient of friction; and (6) phase lag, D3 and D3', which are defined as phase lag between peaks and valleys in normal force and normal displacement. Figure 5 shows the patterns of ΔF_{s1}, ΔF_{s2}, $\Delta\mu_{d1}$, $\Delta\mu_{d2}$, Δd_1, Δd_2, D1, D2 and D3 versus shear displacement under different normalized oscillation amplitude Ɛ.

3.1 Variation of Shear Force ΔF_{s1} and ΔF_{s2}

The measured peak-to-valley value of the shear force fluctuations ΔF_{s1} and ΔF_{s2} show complex patterns influenced by normal load oscillation amplitude and shear displacement. In Fig. 3, the maximum and minimum values of the shear forces decrease with increasing normal load oscillation amplitude. Under large normal load oscillation amplitude, the measured shear force can even have negative values, e.g., negative shear force is measured when A = 40 kN. ΔF_{s1} is larger than ΔF_{s2} in each cycle in an early shearing stage. With ongoing shear displacement, peak and valley values of shear force, ΔF_{s1} and ΔF_{s2}, increase gradually, finally reaching a constant value, where ΔFs_1 is nearly identical to

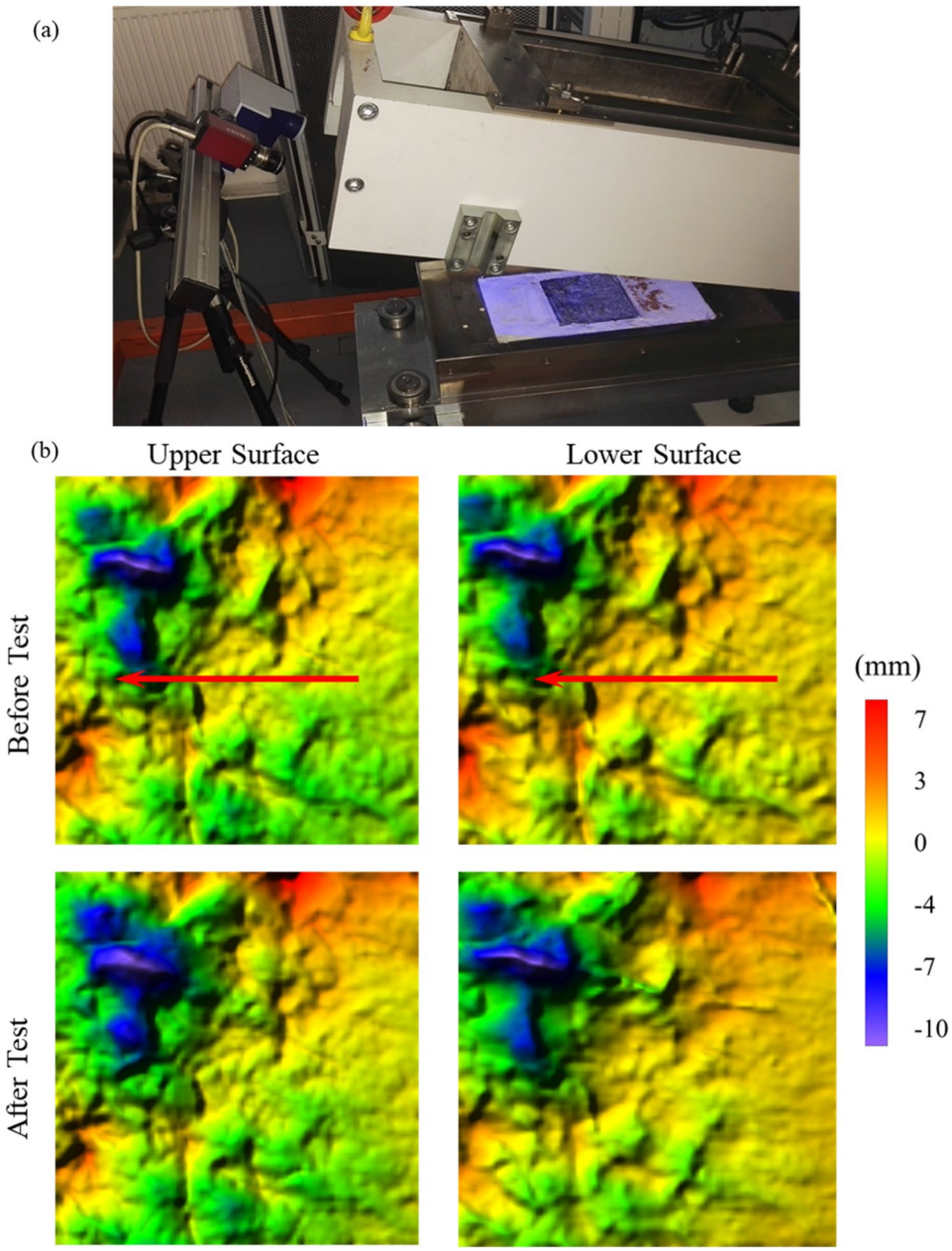

Fig. 2 **a** 3D scanner "z-Snapper". **b** Scanned topography of the rough fracture surface before and after the experiment. The scanned z- coordinate of the upper fracture was converted. Red lines indicate the shear direction

ΔF_{s2}. Figure 5a shows the relationship between the apparent dynamic coefficients of friction ($\Delta F_{s1}/2A$, $\Delta F_{s2}/2A$) and the shear displacement. $\Delta F_{s1}/2A$ and $\Delta F_{s2}/2A$ increase with shearing and increasing normal force oscillation amplitude until A = 30 kN, while, they show a decreasing pattern when A = 40 kN. Besides, the cyclic changes in the shear forces are more serrated instead of sinusoidal.

3.2 Variation of Actual Friction Coefficient $\Delta\mu_{d1}$ and $\Delta\mu_{d2}$

The actual friction coefficient follows the same variation pattern like the shear force, which changes periodically with changes in normal loads. Peak and valley data of the actual friction coefficient grow with ongoing shear displacement. The plot of the coefficient of friction has a fairly regular shape (sinusoidal) until A = 30 kN. A 'dynamic overshooting' happens when A = 40 kN and the sinusoidal friction pattern changes (see Sect. 4.3). Figure 5b illustrates the peak-to-valley amplitudes $\Delta\mu_{d1}$ and $\Delta\mu_{d2}$ determined according to Fig. 4. $\Delta\mu_{d1}$ is larger than $\Delta\mu_{d2}$ in the early stage of shearing. The variation in apparent friction coefficient increases gradually until $\Delta\mu_{d1} = \Delta\mu_{d2}$. For all dynamic test cases, the peak values of the actual friction coefficient are similar to that obtained under CNL conditions, i.e., $f_{dmax} = \mu_{ss}$. The valley values of the actual friction coefficient rise with decreasing

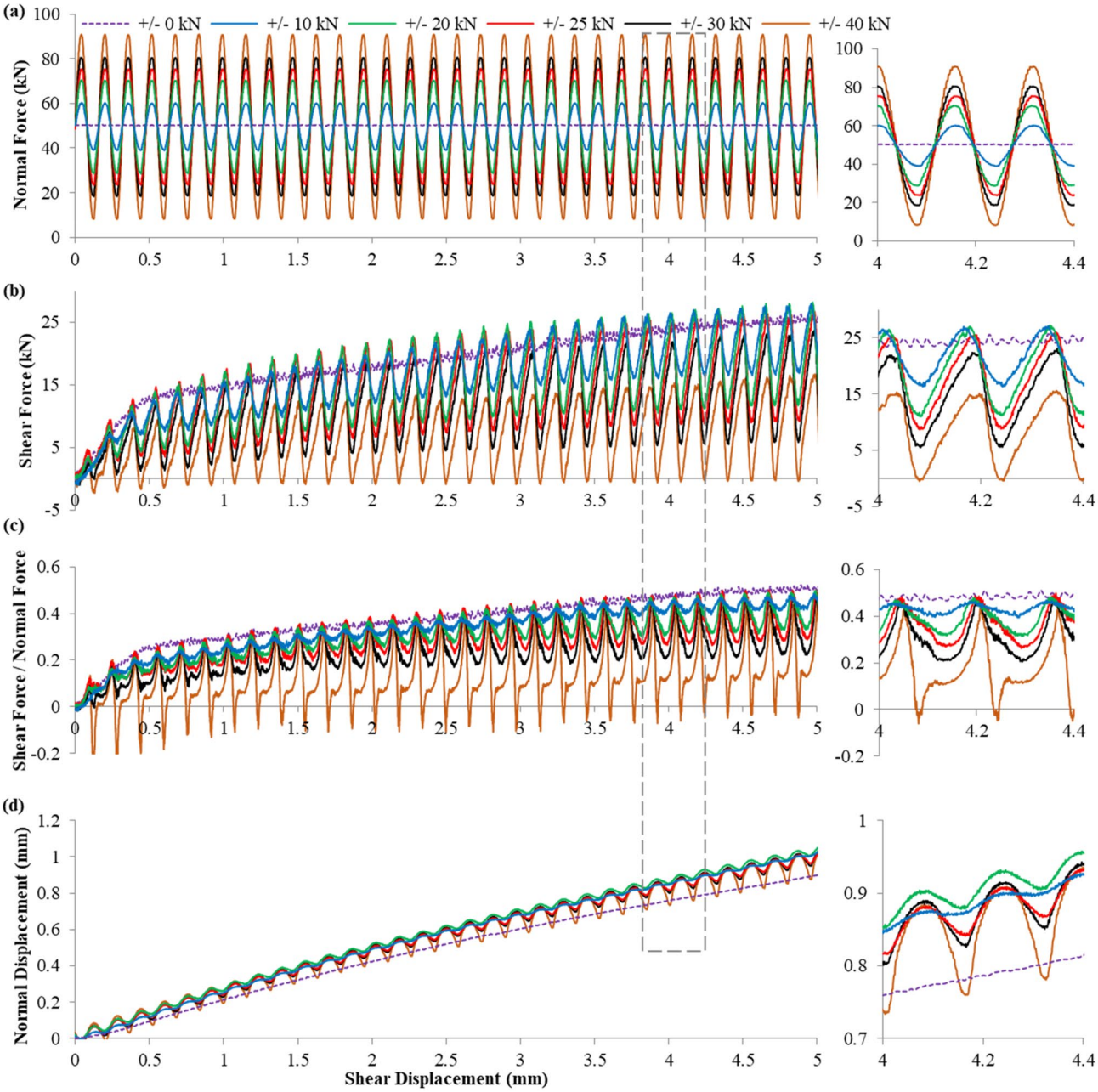

Fig. 3 Experimental results of normal and shear force, actual friction coefficient, and normal displacement as a function of shear displacement for slip rate of 5.0 mm/min, oscillation frequency of 0.5 Hz, initial normal force of 50 kN; dynamic sinusoidal normal forces are $\pm 10, \pm 20, \pm 25, \pm 30$, and ± 40 kN, respectively. ± 0 kN means shear test under constant normal load. The figures on the right are zoom-in of the left ones

normal load oscillation amplitude. $\Delta\mu_{d1}$ and $\Delta\mu_{d2}$ increase with increasing normal load oscillation amplitude.

3.3 Variation of Normal Displacement Δd_1 and Δd_2

As shown in Figs. 3d and 5c the normal displacement under constant normal load shows a nearly linear increase with ongoing shear displacement. In general, the dilation is larger under periodical normal force than that under constant normal force. Both, unloading of normal force and the asperities of the fracture surface promote dilation during the shearing process. For every cycle of loading and unloading, the fracture is compressed and separated in a cyclic manner. During loading, the normal displacement (dilation) is restrained, the separation of the fracture declines and causes enlarged strain at the contact area

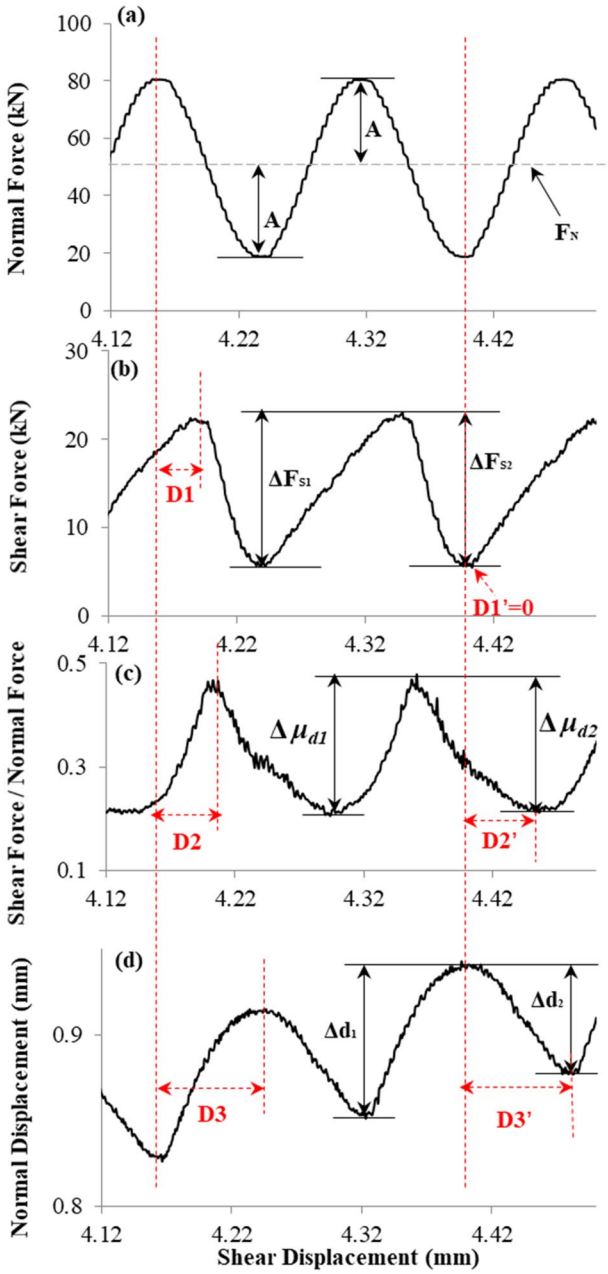

Fig. 4 Quantification of frictional response to oscillating normal loading in the case of A = 30 kN. **a** Changes in normal force. **b** Changes in shear force, ΔF_{s1} and ΔF_{s2} are the peak-to-valley amplitudes of shear load response to normal load vibrations in the loading and unloading stage. Phase lag D1 and D1' are the shear displacement difference between the peaks and valleys of normal and shear force, respectively. **c**) Variation in apparent dynamic friction coefficient, $\Delta\mu_{d1}$ and $\Delta\mu_{d2,}$ are the peak-to-valley amplitudes of the actual coefficient linked to normal load vibrations in the loading and unloading stage. Phase lag D2 and D2' are the shear displacement difference between the peaks and valleys of normal force and coefficient of friction, respectively. **d** Changes of normal displacement, Δd_1 and Δd_2, are the peak-to-valley amplitude normal displacements in relation to normal load vibrations in the loading and unloading stage. Phase lag D3 and D3' are the shear displacement difference between the peaks and valleys of the normal force and normal displacement, respectively

(Greenwood and Williamson, 1966). Only the asperity of the fracture surface promotes dilation, which makes Δd_1 larger than Δd_2 during the cyclic loading. Some irreversible plastic deformations at the contacts also lead the apparent asymmetry between Δd_1 and Δd_2. Moreover, Δd_1 and Δd_2 increase with increasing normal load oscillation amplitude, which has a slight increasing trend with ongoing shear displacement. Δd_1 and Δd_2 consist of three parts: elastic deformation of the fracture as well as the elastic and plastic deformation of the rock matrix (Goodman 1976; Kilgore et al. 2017).

3.4 Phase Lag D1(D1'), D2(D2') and D3(D3')

Perfettini et al. (2001) are the first who theoretically found a time difference between horizontal shear load and vertical load during dynamic oscillations. Then, this theory was proved by laboratory experiments on planar fractures. Boettcher and Marone (2004) observed a time difference between normal and shear load under normal load oscillation frequencies between 0.025 and 2.0 Hz. Dang et al. (2018) found that the time difference is velocity-frequency-amplitude related. However, the above mentioned phase lag pattern changes when fracture roughness is considered.

As illustrated in Fig. 5d–f, the time difference also exists in this study. We observed a time difference between (1) peak vertical force and peak shear force (D1), (2) valley vertical force and valley shear force(D1'), (3) peak vertical force and peak actual friction coefficient (D2), (4) valley vertical force and valley actual friction coefficient (D2'), (5) peak vertical force and peak normal displacement (D3), and (6) valley vertical force and valley normal displacement (D3'). D1 has a slight trend of reduction with ongoing shear displacement, while D2 and D3 remain nearly constant. For different shear positions, the actual coefficient of friction is different (Fig. 3c, the actual friction coefficient increases with ongoing shear displacement), which indicates a phase lag decrease of D1 with increasing actual coefficient of friction. Figure 5d–f show that the relative phase lag of D1 increases with growing normal load oscillation amplitude and decrease with ongoing shear displacement. The relative phase lag of D2 is constant at about 30% in all the tests, which is independent of normal load oscillation amplitude and shear displacement. The relative phase lag of D3 is 50% for all the tests, which means that the variation of vertical settlement changes synchronously with the variation of normal force, consistent with the observations of Kilgore et al. (2017). Time differences between the valleys of normal and shear load, coefficient of friction, and vertical settlement are small, whereas the relative phase lags for D1', D2'and D3' are 0, about 30% and 50%, respectively, nearly constant for all the tests. The magnitude of phase lag of D1 is influenced by the magnitude of shear stiffness (Dang et al. 2016). The shear stiffness increases with increasing joint

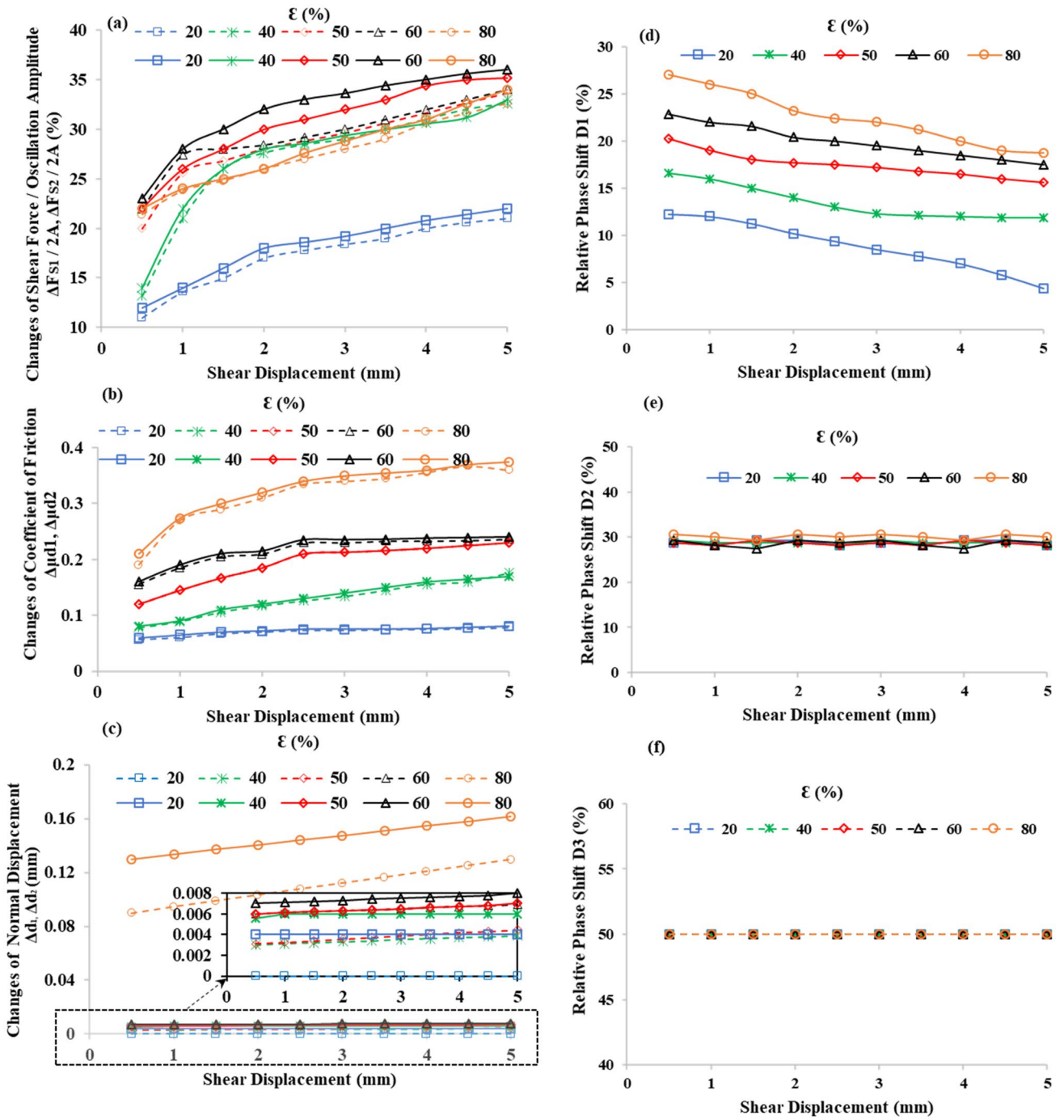

Fig. 5 Influence of normal load oscillation amplitude on shear strength, coefficient of friction, normal load displacement and phase lag. **a** Apparent dynamic friction coefficient ($\Delta F_{s1}/2A$, $\Delta F_{s2}/2A$) versus shear displacement, solid lines denote $\Delta F_{s1}/2A$, dot lines denote $\Delta F_{s2}/2A$. **b** Peak-to-valley amplitudes of actual coefficient of friction ($\Delta\mu_{d1}$ and $\Delta\mu_{d2}$) versus shear displacement, solid lines denote $\Delta\mu_{d1}$, dot lines denote $\Delta\mu_{d2}$. **c** Peak-to-valley amplitudes of normal displacement versus shear displacement, solid lines denote Δd_1, dotted lines denote Δd_2. **d** Details of the time difference between normal force and shear force (D1) versus shear displacement. **e** Details of the time difference between normal force and apparent friction coefficient (D2) versus shear displacement. **f** Details of the time difference between normal force and normal displacement (D3) versus shear displacement

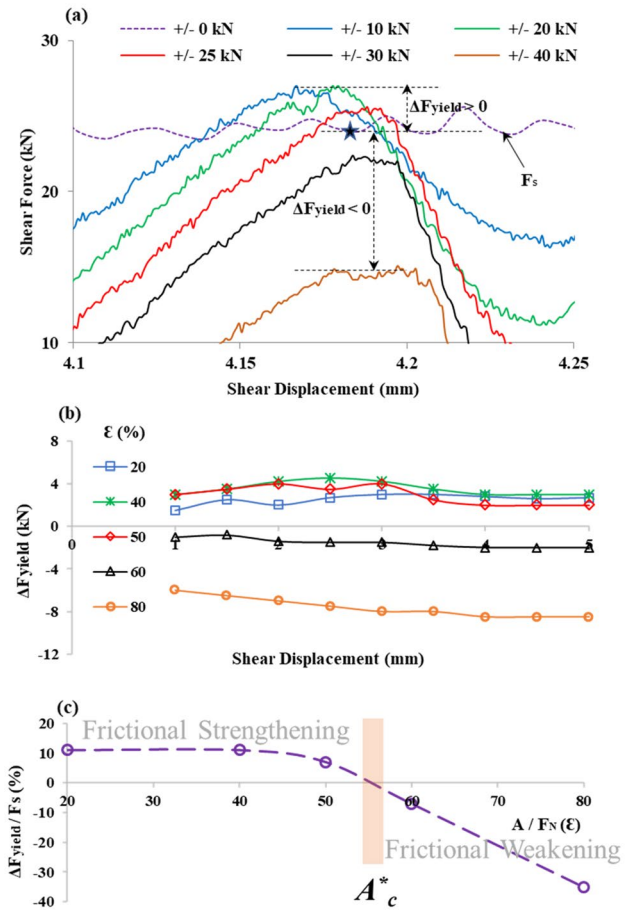

Fig. 6 **a** Definition of ΔF_{yield}. ΔF_{yield} shows positive or negative values, representing strengthening or weakening, respectively. **b** Variation in peak yield strength (ΔF_{yield}) versus shear displacement with different normal force oscillation amplitude. **c** Dynamic fracture strengthening/weakening linked to normal force oscillation amplitude. A critical vibration amplitude A^*_c defined as $\Delta F_{yield}/F_s = 0$ ($A > A^*_c$ indicates induced normal load oscillation-induced weakening, $A < A^*_c$ indicates induced normal load oscillation-induced strengthening)

roughness and stress level (Bandis et al. 1983, Amiri Hossaini et al. 2014). Consequently, the phase lag pattern is different compared to Boettcher and Marone (2004), Dang et al. (2017), when fracture roughness is taken into consideration.

4 Discussion

4.1 Normal Load Oscillation-Induced Strengthening/Weakening

We define ΔF_{yield} as the difference between the maximum friction under the oscillatory normal force and the friction under the constant normal force for the same shear distance. General understanding is that normal load oscillation reduces the shear strength. However, laboratory test results show that ΔF_{yield} (Fig. 6a) can be both: greater than zero or less than zero considering different normal load oscillation amplitudes. Figure 6b shows the influence of oscillation amplitude and shear displacement on ΔF_{yield}. For small oscillation amplitude, $Ɛ < 50\%$, ΔF_{yield} is positive, the peak shear force enhances up to 10% compared to the case of constant normal load. When Ɛ is over 50%, ΔF_{yield} starts to decrease with increasing oscillation amplitude. The peak shear load can be reduced by nearly 40% at an oscillation amplitude of 80%. A critical vibration amplitude A^*_c is defined when $\Delta F_{yield}/F_s = 0$ (Fig. 6c), which separates the entire zone into dynamic fracture weakening ($A > A^*_c$), and dynamic fracture strengthening ($A < A^*_c$). In this study, A^*_c nearly equals 55%. In general, vibrations with large amplitude easily cause normal load oscillation-induced weakening.

The apparent weakening phenomenon documented by the shear strength data, can well be explained using the rate-state friction law (Ruina 1983; Perfettini et al. 2001), which has been effectively applied to simulate frictional sliding of solids and for earthquake events (firstly established for CNL conditions). Linker and Dieterich (1992), Perfettini et al. (2001) extended the rate-state friction law to include variations in normal load, and provided an analytical equation to predict the critical oscillation amplitude. In Perfettini's assumption, the critical amplitude is linked to state variables and fracture stiffness. The normal load oscillation-induced strengthening/weakening is controlled by the loading/unloading rate of normal force, slip rate and fracture stiffness.

4.2 Friction coefficient reduction and shear work

We calculated energy consumption during shearing using the shear force—shear displacement plots, $E = \int_0^{u\,\max} F_s du$, where u is the slip length and F_s is the shear force. The elastic energy of the fracture is not taken into consideration in the present work. The ratio of friction coefficient reduction is the ratio between the minimum friction coefficient under periodical vertical force and the quasi-static friction coefficient, μ_{dmin}/μ_{ss}. Figure 7 shows the shear work and the ratio of friction coefficient reduction under various normal load oscillation amplitudes. A large normal load oscillation amplitude leads to a more serious vibration of the upper block of the sample, which is not beneficial to store the strain energy (Li et al. 2020) in the asperities during shearing. Consequently, the shear work decreases with increasing normal load oscillation amplitude. μ_d/μ_{ss} shows a cyclic behavior, whereby peak and valley values are nearly constant at the same normal load oscillation amplitude. The peak values of μ_d/μ_{ss} are nearly constant during all the tests with a value close to 1, i.e., peak μ_d nearly equals μ_{ss}. The minimum of μ_{dmin}/μ_{ss} increases with reducing the normal

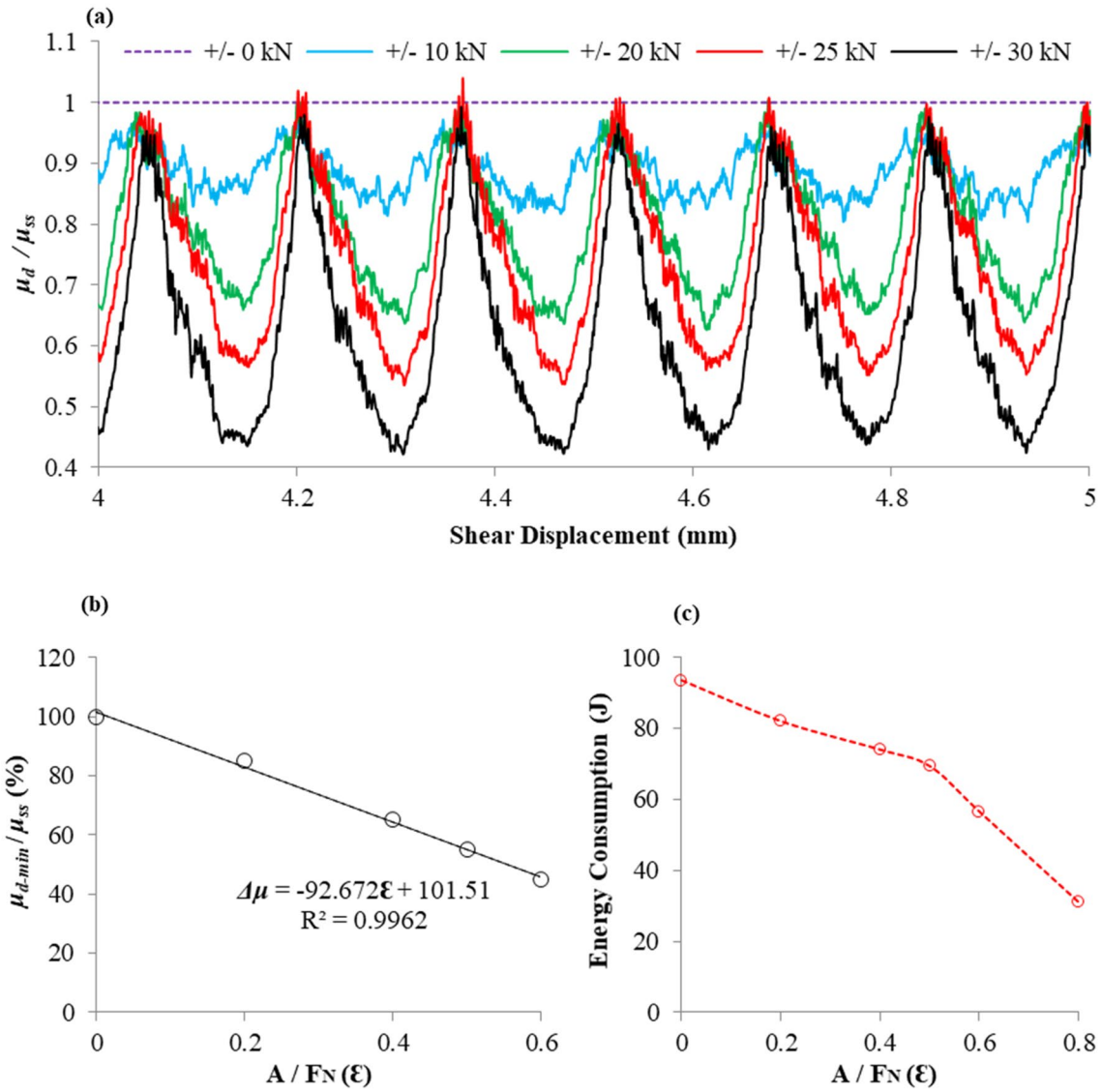

Fig. 7 **a** Dynamic friction coefficient and quasi-static friction coefficient versus shear displacement under normal load oscillation amplitude of $0, \pm 10, \pm 20, \pm 25$ and ± 30 kN, respectively. **b** and **c** Ratio of dynamic friction coefficient reduction and energy consumption versus normalized normal load oscillation amplitude

load oscillation amplitude. The above results indicate that a high normal load oscillation amplitude leads to a lower energy consumption and a large reduction in coefficient of friction, which easily destabilizes the slip. These changing patterns are similar to those documented for planar joints (Dang et al. 2017).

4.3 Interpretation of Negative Shear Force

For direct shear tests with constant slip rate, a negative shear force under a positive normal load seems unreasonable at first glance (shown in Fig. 3, $A = \pm 40$ kN). However, negative shear forces were reliably measured in the case of large dynamic load amplitude (Fig. 8a). Moreover, negative cutting forces are also monitored in Cerchar scratch tests (Zhang 2020).

The apparent friction can reach negative values during tests linked to negative values of shear force. When the rock block is exposed to normal and shear loads, elastic energy is stored due to the elastic deformation. As shown in Fig. 9, the stored energy changes with increasing/decreasing normal load at different shear positions. In the loading stage, (Fig. 9a, b, normal load is F_N and $F_N + A$), elastic energy is stored in the lower block, which reaches the peak value (*E2*) under normal load of $F_N + A$. During unloading, the stored elastic energy releases, the frictional resistance decreases, and the lower block expands (Fig. 9c). The stored elastic energy reaches the minimum

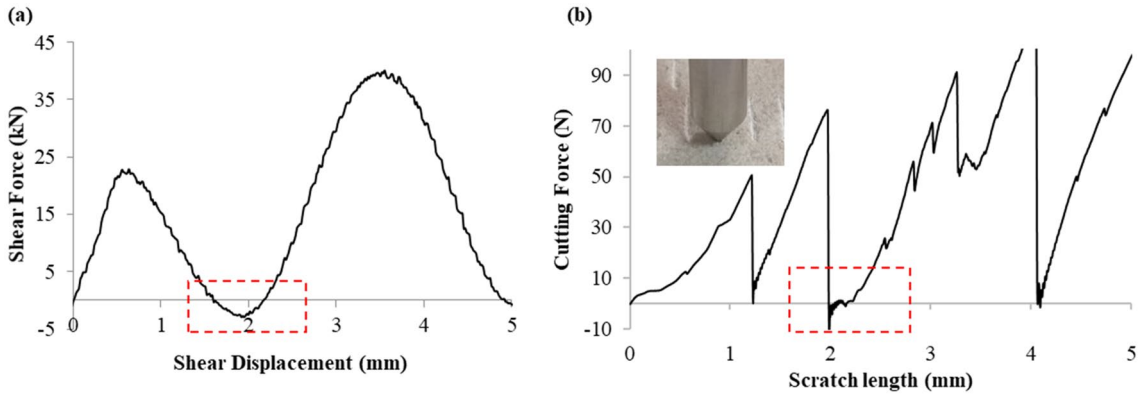

Fig. 8 **a** Additional shear test: shear force versus shear displacement, normal force of 50 ± 40 kN with slip rate of 100 mm/min and loading frequency of 1.0 Hz, **b** Scratch test: cutting force versus scratch length under normal load of 70 N with scratch rate of 20 mm/min. Both of them show temporarily negative shear/cutting forces

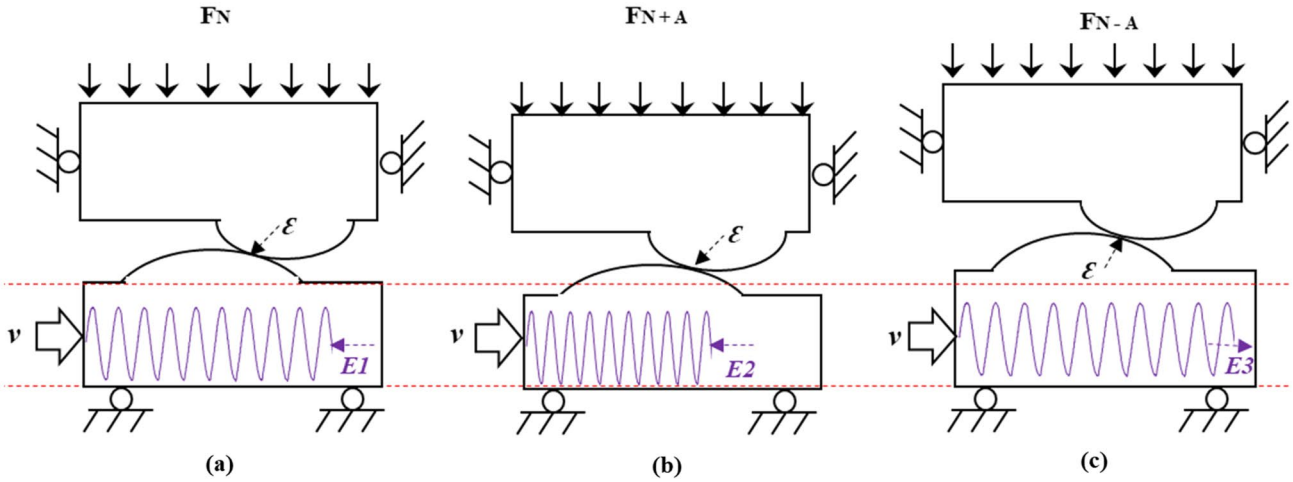

Fig. 9 Schematics of asperity deformation, elastic energy storage and release of the lower block under different normal load conditions. **a** Under normal load of F_N, the lower block is compressed to some extend, the elastic energy is stored, **b** with increasing normal load, the lower block is further compressed, elastic deformation is further accumulated, and stored elastic energy is accumulated reaching the peak values under normal load of $F_N + A$, **c** when normal load becomes smaller, dilation develops, and stored elastic energy is released, a "dynamic overshooting" occurs, stored elastic energy reaches a minimum and dilation reaches the peak value under normal load of $F_N - A$

value (*E3*) under normal load of $F_N - A$. Under normal load of 50 ± 40 kN, the unloading rate of normal force is up to 4800 kN/min (changing from 90 to 10 kN lasts about one second in the laboratory test). This more or less sudden drop in normal force leads to a fast release of elastic energy, a kind of 'shooting' of the lower block combined with a quick drop of the shear force. The expanding rate of the specimen is about 9 mm/min under normal load of 50 ± 40 kN, which is nearly two times larger than the slip rate (5 mm/min). Due to the fast expanding rate, whenever the frictional resistance becomes too low, the lower block may shoot away ('dynamic overshooting', Aboudi and Ryvkin 2014). Consequently, the lower specimen moves faster than the desired (fixed) slip rate, thus the piston has to produce a counterforce (negative force) to maintain the constant velocity. Earthquakes and blasting may induce a fast release/storage of the elastic energy in the rock matrix. If they act on a steady creeping rough fracture, the stress state of the fracture surface becomes very complicated. In some specific cases, apparent friction can become negative.

5 Conclusions

Normal load oscillation amplitude has a distinct influence on the slip behavior of rough rock fractures. In general, a small oscillation amplitude increases the shear strength

and a large oscillation amplitude reduces the shear strength. A critical normal load oscillation amplitude is confirmed to judge the normal load oscillation-induced strengthening or normal load oscillation-induced weakening of a slipping rock fracture. The reduction of the friction coefficient is larger under large normal load oscillationn amplitude. The energy consumption decreases with increasing normal load oscillation amplitude. A time difference between peak vertical force and peak shear force is observed. It rises with rising vertical force oscillation amplitude and decreases with ongoing shear displacement. Our results imply that slipping joints or fractures which experience higher normal load oscillation amplitude react more sensitively.

A limitation of the present research is that damage or plastic deformation of the fracture asperities is not considered. Besides, normal load oscillation frequency, slip rate, water and temperature effect are not yet taken into account, although they may have an influence on the frictional behavior under dynamic normal loading (Boettcher and Marone 2004; Beeler et al. 2019; Dang et al. 2019, 2021).

Acknowledgements This work was supported by the National Natural Science Foundation of China (51904359, 51978677, 52111530089), the Natural Science Foundation of Guangdong Province of China (2020A151501528), the Guangdong Provincial Department of Science and Technology (Grant No. 2019ZT08G090), the Enhanced National Key Basic Research Program (2019-JCJQ-ZD-352-00-04) and Science and Technology Program for Sustainable Development of Shenzhen (KCXFZ202002011008532). Special thanks to Dr. Thomas Frühwirt, who helped to generate the dynamic signals, Mr. Tom Weichmann, who helped to operate the shear box device, and Mr. Gerd Münzberger, who helped to install the samples during laboratory testing. The laboratory test data can be download at https://doi.org/10.6084/m9.figshare.12403538.v1.

Declarations

Conflict of interest The authors declare that they have no conflicts of interest to this work.

References

Aboudi J, Ryvkin M (2014) Dynamic overshooting in 2D periodic materials with square voids caused by sudden flaw appearance. Int J Solids Struct 51(13):2345–2359

Aiken C, Meng X, Hardebeck J (2018) Testing for the 'predictability' of dynamically triggered earthquakes in the geysers geothermal field. Earth Planet Sci Lett 486:129–140

Barton NR, Choubey V (1977) The shear strength of rock joints in theory and practice. Rock Mech 10(1–2):1–54

Beeler NM, McLaskey GC, Lockner D, Kilgore B (2019) Near-fault velocity spectra from laboratory failures and their relation to natural ground motion. J Geophys Res: Solid Earth 125(B2):e2019JB017638

Boettcher MS, Marone C (2004) Effects of normal stress variation on the strength and stability of creeping faults. J Geophys Res: Solid Earth 109(B3):B03406

Bureau L, Baumberger T, Caroli C (2000) Shear response of a frictional interface to a normal load modulation. Phys Rev E 62(5):6810–6820

Candela T, Brodsky EE, Marone C, Elsworth D (2014) Laboratory evidence for particle mobilization as a mechanism for permeability enhancement via dynamic stressing. Earth Planet Sci Lett 392:279–291

Cochard A, Rice JR (2000) Fault rupture between dissimilar materials: ill-posedness, regularization, and slip-pulse response. J Geophys Res: Solid Earth 105(B11):25891–25907

Cochard A, Bureau L, Baumberger T (2003) Stabilization of frictional sliding by normal load vibrations. J Appl Mech 70:220–226

Dang W, Konietzky H, Frühwirt T (2016) Shear behaviour of a plane joint under dynamic normal load (DNL) conditions. Eng Geol 213:133–141

Dang W, Konietzky H, Frühwirt T (2017) Direct shear behavior of planar joints under cyclic normal load conditions: effect of different cyclic normal force amplitudes. Rock Mech Rock Eng 50(4):1–7

Dang W, Konietzky H, Chang L, Frühwirt T (2018) Velocity-frequency-amplitude-dependent frictional resistance of planar joints under dynamic normal load (DNL) conditions. Tunn Undergr Space Technol 79:27–34

Dang W, Konietzky H, Frühwirt T, Herbst M (2020) Cyclic frictional responses of planar joints under cyclic normal load conditions: laboratory tests and numerical simulations. Rock Mech Rock Eng 53:337–364

Dang W, Chen J, Huang L (2021) Experimental study on the velocity-dependent frictional resistance of a rough rock fracture exposed to normal load vibrations. Acta Geotech 16(7):2189–2202

Dang W, Wu W, Konietzky H, Qian J (2019) Effect of shear-induced aperture evolution on fluid flow in rock fractures. Comput Geotech 114:103152

Gong F, Luo S, Lin G (2020) Evaluation of shear strength parameters of rocks by preset angle shear, direct shear and triaxial compression tests. Rock Mech Rock Eng 53:2505–2519

Gong F, Wang Y, Wang Z (2021) A new criterion of coal burst proneness based on the residual elastic energy index. Int J Min Sci Technol 31(4):553–563

Goodman RE (1976) Methods of geological engineering in discontinuous rocks. Int J Rock Mech Min Sci Geomech Abstr 13(10):155

Greenwood JA, Williamson JBP (1966) Contact of nominally flat surfaces. Proc R Soc A 295:300–319

Hobbs BE, Brady BHG (1985) Normal stress changes and the constitutive law for rock friction (abstract). Eos Trans AGU 66:385

Hong T, Marone C (2005) Effects of normal stress perturbations on the frictional properties of simulated faults. Geochem Geophys Geosyst 6:Q03012

Ji Y, Zhuang L, Wu W, Hofmann H, Zang A, Zimmermann G (2021) Cyclic water injection potentially mitigates seismic risks by promoting slow and stable slip of a natural fracture in granite. Rock Mech Rock Eng 54(10):5389–5405

Julian BR (2000) Period doubling and other nonlinear phenomena in volcanic earthquakes and tremor. J Volcanol Geotherm Res 101(1):19–26

Kilgore B, Lozos J, Beeler N, Oglesby D (2012) Laboratory observations of fault strength in response to changes in normal stress. J Appl Mech 79(3):031007

Kilgore B, Beeler NM, Lozos J, Oglesby D (2017) Rock friction under variable normal stress. J Geophys Res: Solid Earth 122(9):7042–7075

Konietzky H, Frühwirt T, Luge H (2012) A new large dynamic rockmechanical direct shear box device. Rock Mech Rock Eng 45(3):427–432

Li Y, Wu W, Wei X (2020) Analytical modeling of the shear behavior of rock joints with two-order asperity dilation and degradation. Int J Geomech 20(6):04020062

Linker MF, Dieterich JH (1992) Effects of variable normal stress on rock friction: observations and constitutive equations. J Geophys Res 97:4923–4940

Marone C (1998) Laboratory-derived friction laws and their application to seismic faulting. Annu Rev Earth Planet Sci 26(1):643–696

Mei C, Barbot S, Wu W (2021) Period-multiplying cycles at the transition between stick-slip and stable sliding and implications for the Parkfield period-doubling tremors. Geophys Res Lett 48:e2020GL091807

Meng F, Wong NYL, Zhou H, Wang Z (2018) Comparative study on dynamic shear behavior and failure mechanism of two types of granite joint. Eng Geol 245:356–369

Mighani S, Bernabé Y, Boulenouar A, Mok U, Evans B (2019) Creep deformation in Vaca Muerta shale from nanoindentation to triaxial experiments. J Geophys Res: Solid Earth 124(8):7842–7868

Molinari A, Perfettini H (2017) A micromechanical model of rate and state friction: 2. effect of shear and normal stress changes. J Geophys Res: Solid Earth 122(4):2638–2652

Olsson WA (1988) The effects of normal stress history on rock friction, key questions in rock mechanics. In: Proceedings of the 29th U.S. Symposium, Univ. of Minnesota, Balkema, pp. 111–117.

Perfettini H, Schmittbuhl J, Rice JR, Cocco M (2001) Frictional response induced by time dependent fluctuations of the normal loading. J Geophys Res: Solid Earth 106:455–472

Prakash V (1998) Frictional response of sliding interfaces subjected to time varying normal pressures. J Tribol 120:97–102

Rice JR (2006) Heating and weakening of faults during earthquake slip. J Geophys Res: Solid Earth 111:B05311

Rice JR, Lapusta N, Ranjith K (2001) Rate and state dependent friction and the stability of sliding between elastically deformable solids. J Mech Phys Solids 49(9):1865–1898

Ruina AL (1983) Slip instability and state variable friction laws. J Geophys Res: Solid Earth 88:10359–10370

Sheng M, Li P, Zhuang XY, Wang JB (2020) Influence of cyclic normal stress on shear friction of EGS granite fractures. Eng Fract Mech 238:107268

Smith SAF, Nielsen S, Toro GD (2015) Strain localization and the onset of dynamic weakening in calcite fault gouge. Earth Planet Sci Lett 413(4):25–36

Stein RS (1999) The role of stress transfer in earthquake occurrence. Nature 402:605–609

Tse R, Cruden DM (1979) Estimating joint roughness coefficients. J Rock Mech Min Sci Geomech Abstr 16(5):303–307

Webber S, Ellis S, Åke F (2018) "Virtual shear box" experiments of stress and slip cycling within a subduction interface mélange. Earth Planet Sci Lett 488:27–35

Wei M, Kaneko Y, Liu Y, Mcguire JJ (2013) Episodic fault creep events in California controlled by shallow frictional heterogeneity. Nat Geosci 6:1–5

Wei M, Liu Y, Kaneko Y, Mcguire JJ, Bilham R (2015) Dynamic triggering of creep events in the Salton Trough, Southern California by regional M≥5.4 earthquakes constrained by geodetic observations and numerical simulations. Earth Planet Sci Lett 427(1):1–10

Xie HP, Zhu JB, Zhou T, Zhao J (2021) Novel three-dimensional rock dynamic tests using the true triaxial electromagnetic hopkinson bar system. Rock Mech Rock Eng 54(4):2079–2086

Zhang G (2020) PhD Thesis: Cerchar abrasivity tests: Laboratory tests and numerical simulations. TU Bergakademie Freberg

Zhou T, Zhu JB, Xie HP (2020) Mechanical and volumetric fracturing behaviour of three-dimensional printing rock-like samples under dynamic loading. Rock Mech Rock Eng 53(6):2855–2864